WORLD CONFERENCE ON TIMBER ENGINEERING 2025
BRISBANE, AUSTRALIA
Advancing Timber for the Future Built Environment

MOMENT JOINTS IN THE MINOR STRENGTH AXIS OF CLT PANELS

Armin Hosseini [1], Md Shahnewaz [2], Carla Dickof [3], Jianhui Zhou [4], Thomas Tannert [5]

ABSTRACT: The structural performance of joints in the minor strength axis of cross-laminated timber (CLT) panels was experimentally assessed using four-point and three-point bending tests. Four different joints were tested: S1) screwed plywood splines; S2) glued plywood splines; S3) T-joints; and S4) X-fix shear keys. The glued splines provided the highest rotational stiffness, while the screwed splines and T-joints exhibited larger ductility. Subsequently, a numerical model, validated by the experiments, was used to evaluate the joint demands. It was shown that increasing the rotational stiffness from 500 to 5000 kNm/rad/m significantly improved floor performance, specifically reducing the deflection by approximately 50%. However, further increases in rotational stiffness only resulted in incremental performance gains.

KEYWORDS: Cross-laminated timber, Rotational stiffness, Self-tapping screws, Spline connection

1 – INTRODUCTION

Mass-timber products have been increasingly used in construction, and cross-laminated timber (CLT) has emerged as the primary product, with floors currently being the main application. CLT is produced by laminating boards in orthogonal cross-layers, creating major and minor strength directions [1]. The most efficient use of CLT is to take advantage of its two-way resistance, where both major and minor directions contribute to the load transfer to the supports, necessitating connections between the individual panels [2].

Due to the dimensional restrictions of press and transportation, i.e. CLT panels are typically produced in widths of 3.0 m or less, connections are required to establish continuity between adjacent panels. Amongst metal dowel-type fasteners, self-tapping screws (STS) have become the preferred choice because they can be installed without predrilling, making STS a cost-efficient solution [3]. The out-of-plane performance of edge-to-edge connections employing STS was shown to provide sufficient strength and stiffness for CLT panel edge connections [4]. Stieb et al. [5] developed a rigid edge connection between two CLT floor panels, by installing STS and grouting the gap with concrete. The study showed that a rotational stiffness exceeding 5000 kNmrad^{-1}m^{-1} had negligible effects on the structural performance.

Besides STS-based edge connections, the proprietary T-joint could serve as a focal point where the heads of multiple STS installed at different angles converge, providing a flush surface with no protruding parts and offering easy positioning in the borehole, enhancing the practicality of its application [6]. An alternative to using STS to is the use of wooden shear keys, such as the X-fix [7]. High in-plane load-carrying capacity and stiffness of X-fix connectors have been shown [8], yet their out-of-plane performance has not been studied. Adhesive joints are a viable alternative to mechanical fasteners. While the most straightforward option is to glue on plywood splines, the proprietary TS3™ system allows for butt-jointing CLT using a two-component polyurethane that can achieve bending strengths up to 21 MPa [9].

The objective of this study was to investigate the out-of-plane performance of connections in the minor strength axis of edge-connected CLT. To achieve this objective, the structural performance of four different connection options were investigated using four-point and three-point bending loading. The secondary objective is to numerically determine the required rotational stiffness to meet the bending moment and shear force demand in these connections when applied to point-supported CLT floor.

2 – EXPERIMENTAL INVESTIGATION

2.1 OVERVIEW

Four types of configurations were tested at the Fast+Epp's Concept Lab in Vancouver: series S1 (screwed-on surface plywood splines); series S2 (glued-on surface plywood splines); series S3 (T-joints utilizing the proprietary connector); and series S4 (X-fix using a wooden shear key with a dovetail shape).

2.2 MATERIALS

In this study, 600 mm wide and 245 mm thick 7-ply (35 mm per layer) CLT of V2M6 grade manufactured by Kalesnikoff in accordance with ANSI/APA PRG 320 [10] was used. For this grade, No.1/No. 2 SPF lumber was used in both longitudinal and transverse layers. The 7-ply panels often

[1] Armin Hosseini, School of Engineering, University of Northern British Columbia, Prince George, Canada, hosseinis@unbc.ca
[2] Md Shahnewaz, Fast + Epp, Vancouver, Canada, mshahnewaz@fastepp.com
[3] Carla Dickof, Fast + Epp, Vancouver, Canada, cdickof@fastepp.com
[4] Jianhui Zhou, School of Engineering, University of Northern British Columbia, Prince George, Canada, jianhui.zhou@unbc.ca
[5] Thomas Tannert, School of Engineering, University of Northern British Columbia, Prince George, Canada, thomas.tannert@unbc.ca

https://doi.org/10.52202/080513-0306

require weak-axis moment connections to satisfy deflection criteria for floors in which the support spacing in the minor strength direction exceeds the panel width. The 7-ply panels provided the opportunity to engage two longitudinal layers (the 4th and the 6th layer) in the load transfer in the the weak-axis moment connections.

As surface splines, 19.1 mm thick Baltic birch plywood, grade B, was used. Fully-threaded Ø8×160 mm and Ø10×320 mm ASSY plus VG screws with a countersunk (CSK) head were utilized [11]. In the glued splines specimens, Ø6×100 mm SK screws with washer head were used to clamp the plywood onto the CLT panels during curing. LePage PL Premium Max, a construction adhesive with a compression shear strength of 9 MPa, an open time of 20 min and a curing time of 24-48 hours, and Titebond III, a wood glue, with an assembly time of 10-15 min, and a minimum shear strength of 5.5 MPa, were used.

2.2 SPECIMEN DESCRIPTION

Series S1 consisted of two plywood sheets attached at the bottom of the CLT panels. In the minor strength direction, the 7th layer does not transfer stresses in bending, yet the continuous splines do. The 400 mm long and 600 mm wide plywood was connected to the CLT using 12 fully-threaded Ø8×160 mm STS on each side, installed at 45º, see Figure 1a.

In series S2, similar to the screwed spline, the 7th layer of the CLT was removed in the connection zone. Two plywood sheets, again 400 mm long, and 600 mm wide, were glued together using Titebond III, and then glued onto the CLT using 175 ml PL Premium Max. 16 washerhead Ø6×100 mm STS were used to clamp the plywood onto the CLT panels during curing. These screws were removed before testing.

In series S3, four D40 W30 T-joints were arranged in a zigzag pattern, spaced 120 mm along the panel width, with two on the left side and two on the right side of the connecting line, as shown in Figure 1b. Each T-joint was attached with two fully-treaded Ø8×160 mm STS on one side at 28˚ to the surface, and one fully-treaded Ø10×320 mm STS at 30˚ on the other side. The T-joints were installed 18 mm recessed into the 7th layer.

Series S4 involved two X-fix type C, 130 mm long, 96 mm wide, and 90 mm deep, to join the panels, as depicted in Figure 1c. The X-fix were spaced 300 mm apart at the center of the panel after removing the 7th layer such that the X-fix engaged the 6th, 5th, and part of the 4th layers of the CLT panel.

2.3 Test set-up

The four-point bending tests, shown in Figure 2a, created pure bending and zero shear at the connections. The length of the two connected panels was 3450 mm, and the span between the supports was 2730 mm. The line loads were applied at a distance of 495 mm from the connection. Simple line supports without constraining rotational movement were provided. Four linear variable differential transformers (LVDTs) were used to measure the mid-span deflection and the connection gap opening.

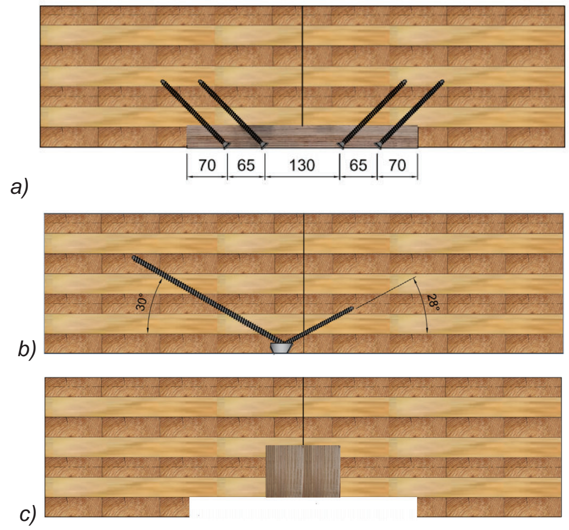

Figure 1. Connections: a) Spline with inclined STS; b) T-joint; c) X-fix

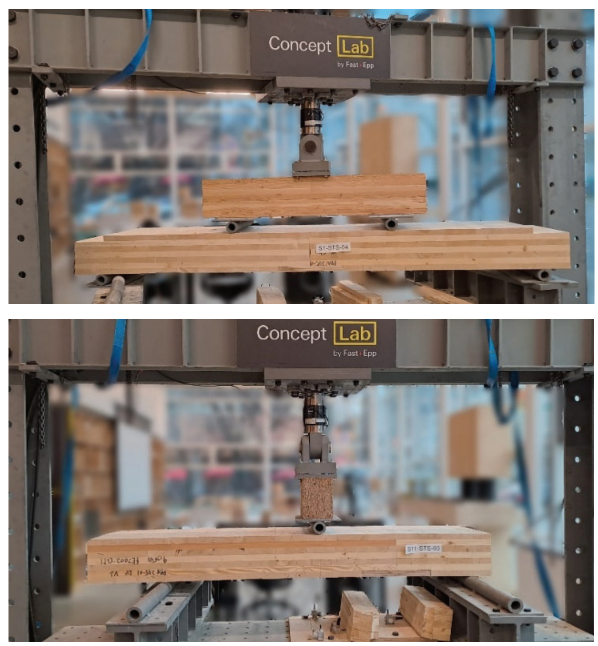

Figure 2. Test set-ups: a) four-point bending test; b) three-point bending test

Three-point bending tests, shown in Figure 2b, were employed to evaluate the connections under simultaneous out-of-plane shear forces and out-of-plane bending moments. The specimen length was 2300 mm, and the span between supports was 1752 mm. The line load was applied at the midpoint of this span and extended along the entire width of the panel. LVDT pairs were installed at center span and the connecting line to record deflections, and to the sides of the connecting line to measure the gap opening of the connection.

2.3 LOADING PROTOCOL AND RESULT METRICS

All testing followed a modified ISO 6891 [12] loading protocol, at a displacement-controlled rate of 8 mm/min. The load was applied with a hydraulic actuator and recorded with a calibrated load cell. The bending moment capacity (M_{ult}) was determined from the peak load. The serviceability rotational stiffness (C_{φ}) was defined from the slope of the moment-rotation curve in the range of 10% to 40% of the peak load. The rotation was represented by the gap angle opening of the connection. Ductility (μ) was defined as the ratio of ultimate displacement, d_{ult}, to yield displacement, d_Y. The displacement d_Y was determined using ISO 6891 [12] and d_{ult} represents the deflection corresponding to the point where the load drops to 80% of the peak load. Ductility was evaluated with the scale proposed by Smith et al. [13]: brittle ($\mu \leq 2$), low ductility ($2 \leq \mu \leq 4$), moderate ductility ($4 \leq \mu \leq 6$) and high ductility ($\mu > 6$).

3 – EXPERIMENTAL RESULTS

3.1 FOUR-POINT BENDING LOAD-DEFLECTION

Representative load-displacement curves of specimens from each connection configuration are shown in Figure 3. In the screwed spline samples (S1), performance was characterized by three stages: a linear part, a nonlinear part with reduced stiffness leading up to the peak load, and a gradual drop in load-carrying capacity until failure. The load-deflection characteristics of glued spline connections (S2) exhibited linear behavior up to peak loads, immediately followed by brittle failure. The load-deflection curve of the T-joint (S3) can be divided into three distinct segments: an initial linear phase, a subsequent phase characterized by reduced stiffness leading up to peak loads, and a final segment characterized by a descent until failure. The load-deflection response of the X-fix (S4) was initially almost linear, followed by a gradual decrease in slope.

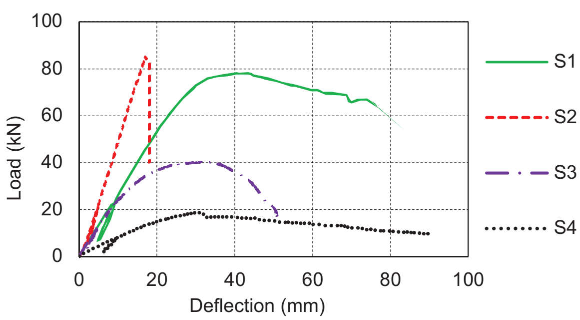

Figure 3. Load-deflection four-point bending tests

3.2 FOUR-POINT BENDING FAILURE MODES

Representative failed specimens are shown in Figure 4. The screwed spline samples (S1) failed mostly in screw withdrawal. In all glued spline samples (S2), failure was confined to the interface between the spline plate and the CLT panels. Failure was abrupt, without notable warnings and did not exhibit any slip between plywood and CLT. Failure in T-joint connections (S3) exhibited three distinct failure modes: i) crushing perpendicular to the grain where T-joints meet the CLT interface; ii) withdrawal of the two short STS; and iii) bending of the STS close to the CLT surface due to the joint rotation. X-fix connections displayed shear failure parallel to the grain throughout the entire height of the X-fix and shear failure perpendicular to the grain in the 5^{th} layer.

a)
b)
c)
d)

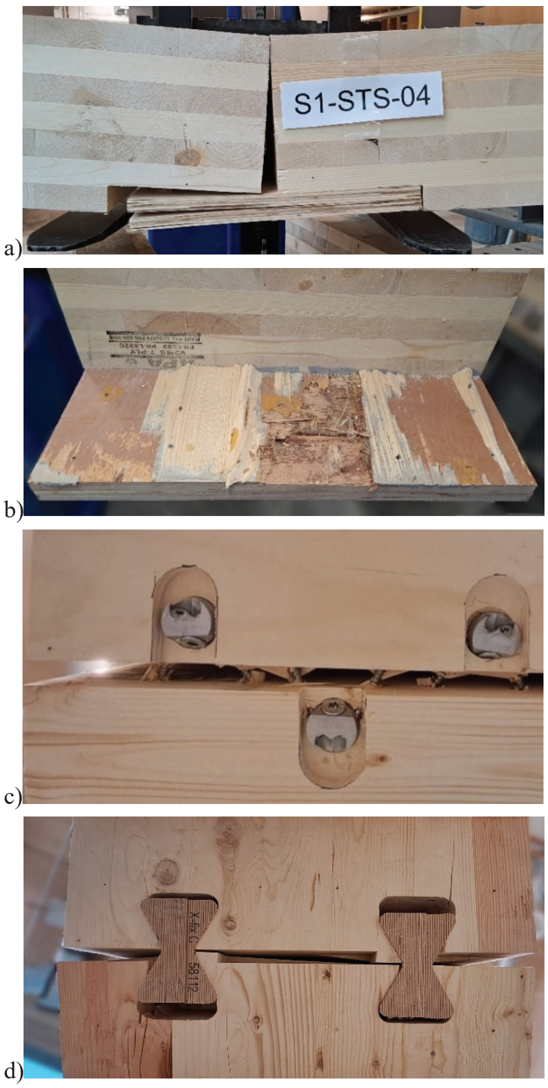

Figure 4. Failure modes four-point bending: a) S1, b) S2, c) S3, d) S4

3.3 FOUR-POINT BENDING TEST ANALYSES

The average values and coefficient of variation (CoV) for the bending moment capacity (M_{ult}), deflection at capacity (d_{ult}), rotational stiffness *(C_{φ})*, and ductility (μ) are summarized in Table 1. The glued spline joints (S2) exhibited the highest

https://doi.org/10.52202/080513-0306

bending moment capacity, followed by the screwed spline, T-joint, and X-fix, with M_{ult} values reaching 94%, 47%, and 23% relative to that of series S2, respectively. Series S2 samples also exhibited superior rotational stiffness with 47,800 $kNmrad^{-1}$. Connections S1 and S3 reached roughly 3,400 $kNmrad^{-1}$ and 2,500 $kNmrad^{-1}m^{-1}$, respectively. Conversely, S4 (X-fix) connections reached rotational stiffness values less than 1,000 $kNmrad^{-1}$ m^{-1}. In terms of ductility, the series involving screws (S1 and S3) as well as the X-fix exhibited limited ductility; however, these series exhibited greater deformation capacity compared to S2, which was brittle.

Table 1: Results from four-point bending tests, average values and CoV

Series	S1 (STS)	S2 (Glue)	S3 (T-joint)	S4 (X-fix)
Replicates	6	6	6	3
M_{ult} [kNm]	33.3	35.5	17.1	8.1
	4%	9%	7%	7%
d_{ult} [mm]	42.2	19.7	31.3	30.0
	14%	14%	14%	2%
C_φ [$kNmrad^{-1}m^{-1}$]	3,555	47,834	2,476	853
	34%	54%	32%	33%
μ [-]	2.3	1.0	3.2	2.2
	21%	0%	20%	15%

3.4 THREE-POINT BENDING LOAD-DEFLECTION

Typical load-deflection characteristics resulting from three-point bending tests on screwed spline (S1), glued spline (S2), and T-joint (S3) connections are presented in Figure 5. S1 had an initially linear response, followed by a nonlinear part developed up to peak load. S2 exhibited a purely linear behavior until reaching an average peak load coinciding with a sudden and abrupt failure. S3 encompassed a linear segment, a second segment with reduced stiffness up to peak load, and a gradual decline in load.

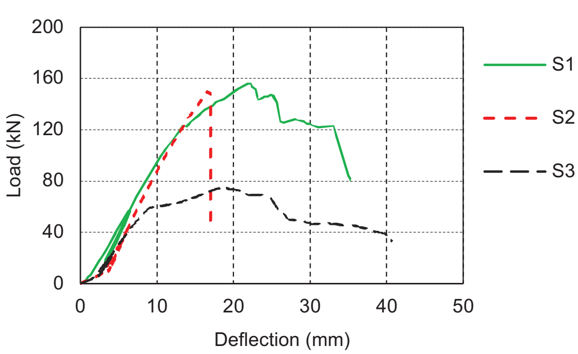

Figure 5. Load-deflection three-point bending tests

3.5 THREE-POINT BENDING FAILURE MODES

Representative failed specimens are shown in Figure 6. For S1, failure was typically accompanied by delamination of the CLT panel, occurring either at the top or bottom of the third layer. For S2, upon reaching the peak load, there was a sudden failure in the plywood and CLT interface, involving a mix of shear failures in solid wood and plywood lamella. In S3, a horizontal crack appeared on the compression side of the second layer at the connecting line, attributable to the low out-of-plane shear resistance of the connection.

a)
b)
c)
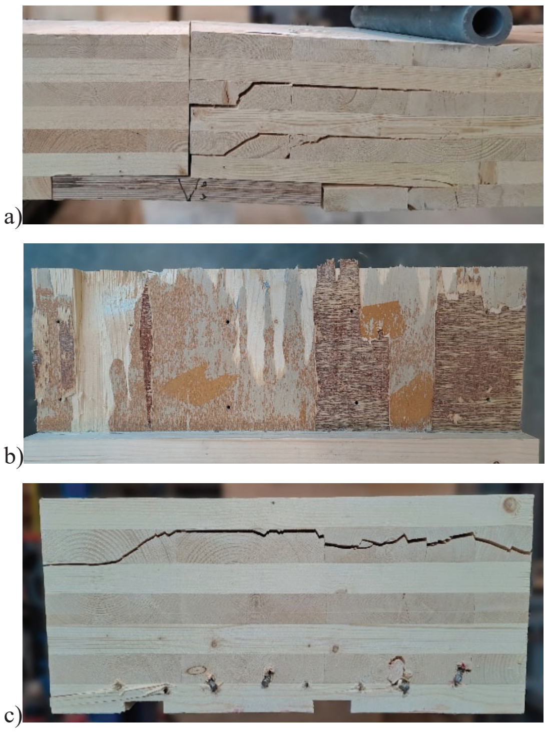

Figure 6. Failure modes three-point bending: a) S1, b) S2, c) S3

3.6 THREE-POINT BENDING TEST ANALYSES

The results are summarized in Table 2: V_{ult} (out-of-plane shear resistance), M_{ult} (bending moment), and rotational capacity C_φ. S1 reached the highest shear force and bending moment resistance, exceeding that of S2 and S3 by 77% and 47%, respectively. The rotational stiffness, C_φ, for series S1 and S3 were about 20% and 9% of S2.

Table 2: Results from three-point bending tests, average values and CoV

Series	S1-STS	S2-Glue	S3-T-joint
V_{ult} [kN]	75	57.5	19.6
	8%	17%	9%
M_{ult} [kNm]	32.8	26.2	15.4
	8%	18%	9%
C_φ [$kNmrad^{-1}$]	6,649	32,533	2,869
	21%	56%	30%

https://doi.org/10.52202/080513-0306

4 – NUMERICAL INVESTIGATIONS

4.1 MODEL DEVELOPMENT

The numerical investigation aimed to determine: i) the demand on the joints between adjacent CLT panels; and ii) the floor performance in the minor direction as a function of joint rotational stiffness.

In Canada, common widths of CLT panels are 2.4 m and 3.0 m. Based on this, three floor layouts, 7.2 m × 7.2 m, 7.2 m × 9.0 m and 9.0 m × 9.0 m, were modelled with the typical CLT floor layups (5-ply and 7 -ply) [14]. Herein the results from floor with dimensions of B×L of 9.0 m × 9.0 m as the most demanding situation are presented. The floors consisted of three CLT panels, grade V2, connected along the minor direction throughout the length of the panels (*L*) and supported on areas 300 mm × 300 mm, which were located in the middle of the side panels along the major direction at a distance (*e*=1.0m) from the edge, see Figure 7. Consequently, the span between point supports was 7.0 m in the major direction and 6.0 m in the minor direction.

Uniform dead and live loads (*DL* and *LL*) were applied, with the load combinations for the ultimate limit state (ULS) and serviceability limit state (SLS) according to NBCC [15]. A *LL* of 2.4 kPa was considered for office buildings, accompanied by a *DL* of 1.0 kPa, excluding the self-weight of the CLT panels, which was also considered in analysis. The floors were designed to meet deflection limits: *L*/180 for total loads and *L*/360 for live loads as outlined in NBCC [15]. Stiffness values of 500, 1,000, 1,500, 2,000, and 5,000 kNmrad^{-1}m^{-1}, and a continuous panel representing an infinite value were selected.

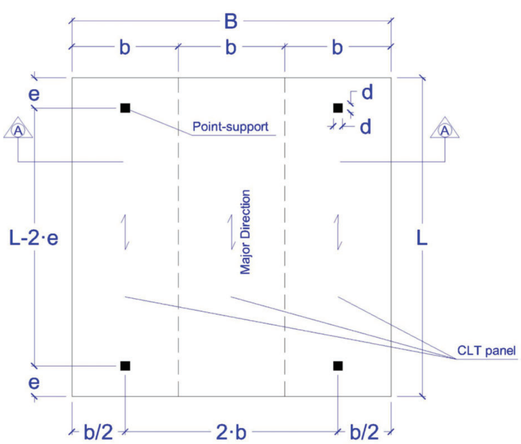

Figure 7. Modelled floor plan

The numerical models were developed in the software RFEM [20], employing planar orthotropic shell elements and the RF-Laminate module for CLT. The CLT panels were 245 mm thick, composed of seven 35 mm laminates. The CLT grade was V2M6, indicating the composition of major and minor layers as No. 1/No. 2 SPF, with a modulus of elasticity of 9500 MPa and a specified bending strength of 11.8 MPa [17]. The point supports were modelled by restraining all translational and rotational degrees of freedom of a 300 mm × 300 mm surface. The connections between two adjacent CLT panels were modeled using line releases which allow for structural decoupling of objects connected to a line, translational springs in the three local axes directions and a rotational spring about the longitudinal line axis to simulate the semi-rigid connection between the two connected surfaces for shear and moment transfer. The model was validated by comparing the numerical results to the experimental load–displacement curves of series S1 for both four-point and three-point bending tests.

4.2 NUMERICAL RESULTS

A sensitivity analysis of rotational stiffness was conducted on bending moment and shear force demand at the edge connections as well as on ULS and SLS panel utilizations. Rotational stiffness did not have any effect on the internal out-of-plane shear force. Increasing the column edge distance (*e*) promoted a more uniform distribution of bending moments along the connecting line, as shown in Figure 8.

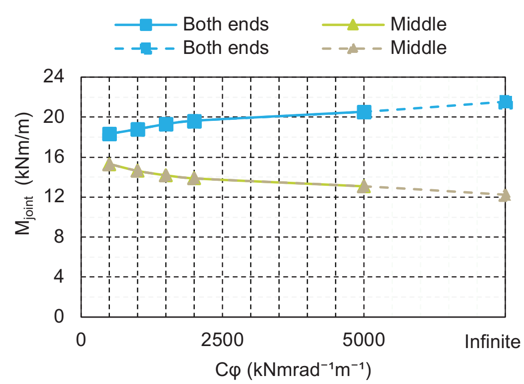

Figure 8. Impact of Cφ on bending moment at connecting line

The impact of rotational stiffness on the ULS utilization (ratio of maximum bending moment to bending moment resistance according to CSA O86 [17] was shown to be relatively small [14]. In contrast, the SLS utilization is highly sensitive to rotational stiffness, particularly at lower values, see Figure 9. Small increments in rotational stiffness result in substantial enhancements. However, this effect diminishes, once a rotational stiffness of around 5,000 kNmrad^{-1}m^{-1} is reached, when the influence of rotational stiffness becomes inconsequential on the floor SLS utilization.

In other words, the floor deflection decreases by approximately 50% when the rotational stiffness is increased from 500 kNmrad^{-1}m^{-1} to 2,000 kNmrad^{-1}m^{-1}. Another reduction in deflection of about 10% is achieved when increasing to connection rotational stiffness to 5,000 kNmrad^{-1}m^{-1}, and an increase towards a rigid joint only provides a further 10% reduction in floor deflection.

https://doi.org/10.52202/080513-0306

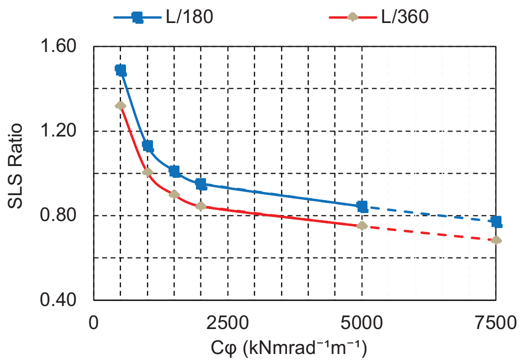

Figure 9. Impact of Cφ on SLS utilisation

5 – CONCLUSION

The out-of-plane structural performance of screwed plywood splines, glued plywood splines, T-joints, and X-fix connections in the minor strength direction of edge-connected CLT floor segments was assessed. The results can be sumamrized as follows:

1. The required rotational stiffness for point-supported CLT floors in the minor axis to limit deflection was determined as 5000 $kNmrad^{-1}m^{-1}$, with higher stiffness not offering added benefit.
2. However, large rotational stiffness increases bending moments at both connection ends, potentially requiring extra connectors.
3. Splines with 17 Ø8×160 mm STS meet target demands for a 9 × 9 m point-supported floor with 3 m wide panels under a 2.4 kPa live load.
4. Glued splines provide ten times the required stiffness for serviceability but fail in a brittle manner.
5. T-joints meet target demands, but optimal STS number and length require further study.
6. The X-fix connector shows moderate ductility but lacks sufficient stiffness and bending capacity for out-of-plane moment connections.

Future research should explore a wider performance spectrum, including large-scale tests on two-way loading, floor vibrations, and combined in-plane and out-of-plane loading to assess diaphragm behavior.

ACKNOWLEDGEMENTS

The project was supported by the Natural Sciences and Engineering Research Council of Canada (NSERC) through an Alliance grant. The support by Fast + Epp's Concept Lab manager Brandon Sullivan, and technician Bernhard Zarnitz is appreciated.

REFERENCES

[1] R. Brandner, G. Flatscher, A. Ringhofer, G. Schickhofer, A. Thiel, Cross laminated timber (CLT): overview and development, Eur. J. of Wood and Wood Products 74 (2016) 331–351.

[2] H. Ganjali, T. Tannert, Md. Shahnewaz, C. Dickof, C. Slotboom, M. Popovski, Punching-shear strength of point-supported CLT floor panels. INTER, Paper 56-12-3, Biel, Switzerland, 2023.

[3] P. Dietsch, R. Brandner, Self-tapping screws and threaded rods as reinforcement for structural timber elements – A state-of-the-art report, Constr Build Mater 97 (2015) 78–89.

[4] J. Asselstine, F. Lam, C. Zhang, New edge connection technology for cross laminated timber (CLT) floor slabs promoting two-way action, Eng Struct 233 (2021) 111777.

[5] T. Stieb, B. Maurer, M. Bestler, P. Dietsch, R. Maderebner, Solutions for edge connections to build two-way spanning cross laminated timber slabs, In: WCTE, Oslo, Norway (2023).

[6] ETA-19/0628 KNAPP T-JOINT connectors, European Technical Assessment, 2022.

[7] ETA-18/0254, X-fix C, European Technical Assessment, (2020).

[8] G.S. Ayansola, T. Tannert, High capacity wooden connector for CLT shear walls, In: World Conference on Timber Engineering, Santiago, Chile (2021).

[9] S. Zöllig, A. Frangi, S. Franke, M. Muster, Timber Structures 3.0 - New Technology for Multi-Axial, Slim, High Performance Timber Structures, In WCTE, Vienne, Austria (2016).

[10] ANSI/APA PRG 320-2019: Standard for Performance-Rated Cross-Laminated Timber, APA – Engineered Wood Association, American National Standard Institute, New York, NY, 2019

[11] CCMC 13677-R SWG ASSY VG Plus and SWG ASSY 3.0 self-tapping wood screws. Canadian Construction Materials Centre, Ottawa, ON, 2013.

[12] ISO 6891-1983. Timber structures: Joints made with mechanical fasteners: General principles for the determination of strength and deformation characteristics. ISO. Geneva, Switzerland, 1983.

[13] I. Smith, A. Asiz, M. Snow, I. Chui, Possible Canadian/ISO approach to deriving design values from test data, In: 39th CIB W18, 2006

[14] Hosseini A, Shahnewaz Md, Zhou J, Tannert T (2025) Structural performance of CLT moment connections in the minor strength axis. Engineering Structures; 328 (2025) 119788.

[15] National Research Council of Canada (NRCC), National Building Code of Canada 2020, Canadian commission on building and fire codes, Ottawa, ON, 2020.

[16] Dlubal Software, https://www.dlubal.com.

[17] Canadian Standards Association (CSA), O86-19 Engineering Design in Wood Standard, CSA Group, Mississauga, ON, 2019.

https://doi.org/10.52202/080513-0306